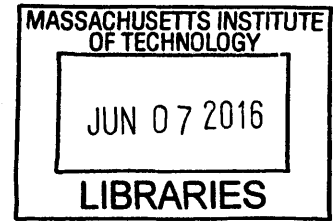# Geometrical Optimization of Arched Structures under Stochastic Loading

By

Daniel Bradley Brownfield

B.S. Civil Engineering
United States Military Academy, 2015
Second Lieutenant, United States Army

Submitted to the Department of Civil and Environmental Engineering
In Partial Fulfillment of the Requirements for the Degree of

Master of Engineering in Civil and Environmental Engineering

at the

MASSACHUSETTS INSTITUTE OF TECHNOLOGY

June 2016

© 2016 Daniel Bradley Brownfield. All Rights Reserved.

The author hereby grants MIT permission to reproduce and distribute publicly paper and electronic copies of this thesis document or in part any medium now known or hereafter created.

Signature of Author:_____ Signature redacted
Department of Civil and Environmental Engineering
May 13, 2016

Certified by:_____ Signature redacted
Corentin Fivet
Lecturer of Civil and Environmental Engineering
Thesis Co-Supervisor

Certified by:_____ Signature redacted
John Ochsendorf
Class of 1942 Professor of Civil and Environmental Engineering and Architecture
Thesis Co-Supervisor

Accepted by:_____ Signature redacted
Heidi M. Nepf
Donald and Martha Harleman Professor of Civil and Environmental Engineering
Chair, Departmental Committee for Graduate Program

Geometrical Optimization of Arched Structures under Stochastic Loading

By:

Daniel Bradley Brownfield

Second Lieutenant, United States Army

Submitted to the Department of Civil and Environmental Engineering
On May 13, 2016, in partial fulfillment of the requirements for the
Degree of Master of Engineering in Civil and Environmental Engineering

Abstract

This thesis presents a method for determining the moment-optimized shape $y(x)$ for arched structures under unpredictable loading scenarios. A frame geometry optimization derivation is presented that demonstrates the relationship between certain unpredicted loads and an equivalent guaranteed loading condition that is more easily solvable through standard equilibrium analysis. The relationship is then broadened to generate the geometric form for arches experiencing randomly applied point loads over continuous intervals. The conclusions from the frame derivation and subsequent applications are summarized in a generalizable conjecture regarding stochastic loading, which states that the moment-optimized arch geometry $y_1(x)$, when subjected to a random point load P with a likelihood of occurrence determined by a probability density function $f(x)$, is equal to the zero-moment solution $y_2(x)$ for an arch subjected to a distributed load $u(x)$ when $f(x) = u(x)$. The conjecture is further reinforced by form-finding models programmed to minimize maximum moments under stochastic loading using structural analysis software. Conceding an extensive range of applicability, this relationship is a direct asset when considering the design of structures subjected to projectile impacts, the location of which are oftentimes unpredictable. As such, an in-progress military shelter development project is examined as a case study to demonstrate the practicality of the theorem.

Key terms: Stochastic Loading Conjecture, stochastic load case, form-finding

Thesis Co-Supervisor: Corentin Fivet
Title: Lecturer of Civil and Environmental Engineering

Thesis Co-Supervisor: John Ochsendorf
Title: Class of 1942 Professor of Civil and Environmental Engineering and Architecture

Acknowledgements

Crafting this thesis without the reliable, heartening counsel of my advisor Corentin Fivet seems unimaginable. Professor John Ochsendorf's contributions also extend well past ever-insightful thesis critiques to include mentorship and reassurance, always timed perfectly to help ease frustrations and regain perspective. I am blessed to have worked alongside these two great men.

I am thankful for the "tough love" of my mentor Professor Christopher Conley, who ensured I began my graduate studies striving for both academic knowledge and personal growth. I am also indebted to my colleagues from the Natick Labs, Karen Horak and Lisa King-Schiappa, who willingly embraced my involvement with their design project for the case study.

Lastly, my gratitude to Dr. Andrew Rich and the members of the Harry S. Truman Scholarship Foundation is immense. Were it not for their mentorship, and friendship, graduate study would have been nothing but a distant fantasy.

Table of Contents

1. Stochastic Loading: An Introduction

The rationale behind examining a load case with a random probability of occurrence stems in part from considering the design goals of defensive military shelters, as the impact location of projectile loads oftentimes cannot be precisely predicted. The term stochastic, originating from the Greek *stokhastikos*, meaning 'aim at, guess,' is defined as "randomly determined; having a random probability distribution or pattern that may be analyzed statistically but may not be predicted precisely" (Merriam-Webster). The term *stochastic load* will refer to such load scenarios in the following chapters.

1.1 Simplifying Assumptions

Soldiers in current operating environments are often subjected to direct and indirect fire even when inside the defensive perimeter of their basecamp. The impact loading scenarios that occupied shelters could encounter inside operational basecamps are infinite. Indirect fire could originate from any surrounding location within a radius of relevant weapon capabilities. Even if a structural design considers only a standardized magnitude of pressure for the design blast, the location and orientation of the resulting forces would be unpredictable. Applying several simplifications to this loading scenario allows for an exploration of the structural behavior of defensive shelters and other structures exposed to similar randomly positioned loading conditions.

Table 1.1 Assumptions used.

Geometric stiffness	*The following derivations seek to determine optimized geometries independent of material properties. As such, only geometric stiffness will be considered.*
Arched Structures	*Many military shelters are arches, or can be modeled as such. Our analyses therefore will consider two-hinged symmetric arches.*
Point Load	*Impacts will be considered as single point load acting in the direction of gravity. This approximation is suitable for certain impact loads (Alves, 2005).*
Large Magnitude	*The magnitude of the point load is large enough relative to the self-weight of the arch that the self-weight may be neglected.*
Stochastic No. 1	*The point load may occur at any location along the length of the arch, or at specified intervals for certain examples.*
Stochastic No. 2	*The odds of indirect fire hitting the exact location more than once are small. Therefore, the modeled load will occur at one location only.*
Stochastic No. 3	*The likelihood of the load's location is either fully random along the specified interval or defined by a probability density function.*

9

1.2 Key Terms and Notation

The following terminology will be referenced extensively throughout the following derivations.

- o *Stochastic Load* – a load which can be applied along a pre-defined length L from a to b while the precise point of application is unknown and has a fully random probability of occurrence along L
- o *Probability Density Function* – a function $f(x) = P_r[a \leq l \leq b]$ that describes the likelihood of occurrence at x for a stochastic load over the support from a to b
- o *Weighted Stochastic Load* – a stochastic load which has a variable probability of occurrence along L defined by a probability density function $P_r[a \leq l \leq b]$
- o *Stochastic Reactions* – an expression that represents likelihood of occurrence of the true reactions, determined through static equilibrium of a weighted stochastic load section cut
- o *Diagram display* – throughout this thesis the following notation will be used to depict various stochastic loading scenarios:
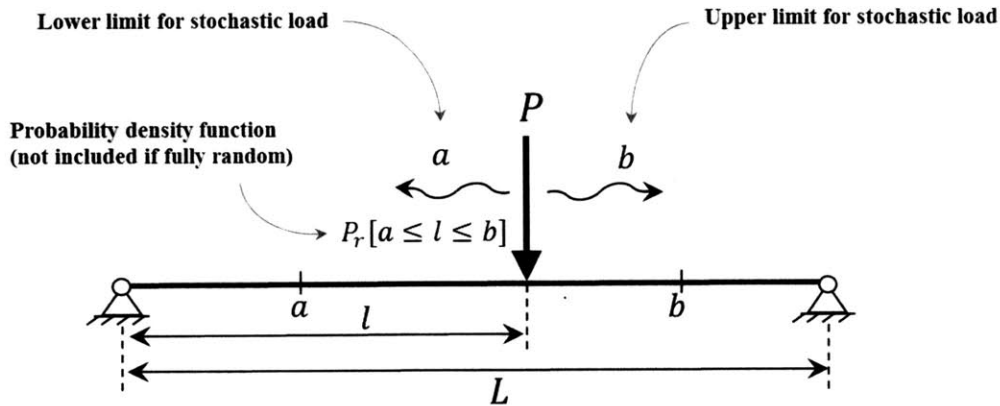

Figure 1.1

The above figure shows that a given point load P will occur somewhere between points a and b, with the probability of the location of that occurrence governed by a specified probability density function $P_r[a \leq l \leq b]$.

1.3 Literature Review

Structural optimization merges mechanics, calculus, and programing techniques to achieve more efficient designs for structures. The field originated as early as 1670 when Robert Hooke first studied the mathematical properties of the catenary curve, the equation for which was later derived by Gottfried Leibniz, Christian Huygens, and Johann Bernoulli in 1691 (Lockwood, 1961). Identifying the relationship between the change in slope and the arc length of the curve gave rise to a mathematical process from which funicular geometries subjected to various distributed loads can be found.

This thesis combines the derivation techniques for optimizing bending moments with probabilistic design. Alejandro Diaz and Martin Bendsoe used probabilistic design and optimization to consider truss configurations under multiple load configurations applied individually (Diaz 1992). They considered sum of the weighted average of the structural responses for each individual loading condition. Constraining parameters such as the overall structure dimensions, this collection of possible responses was optimized for volume of used material using mathematical programming techniques. The approximated solutions were then used to choose similar, more traditional truss configurations. This technique of considering the weighted average of the possible applied loads will be cited later in this thesis when discussing stochastic loads with varying probabilities of occurrence. While various authors have studied structural topology optimization through the lens of probabilistic design, my research into the relevant literature indicates that no one has presented a definitive relationship between geometries optimized for certain stochastic load cases and associated guaranteed loading conditions. As such, this thesis will address that topic.

2. Frame Geometry Optimization

2.1 Introduction and Methodology

The unpredictable nature of stochastic loads necessitates the identification of an equivalent guaranteed loading condition where the structural response of a model may be approximated through standard equilibrium analysis. Assuming that the positions x throughout a length L of the structure where the stochastic load could conceivably be applied are continuous, this equivalent loading condition must take the form of some unidentified distributed load $u(x)$ applied along length L. To identify the relationship between the stochastic load and the equivalent loading condition, we first consider the following simplified frame example. A frame with pinned supports and dimensions as shown below has an equal probability of experiencing either load configuration A or B, but will never experience both simultaneously. The generalized moment distributions for the possible loading scenarios are indicated.

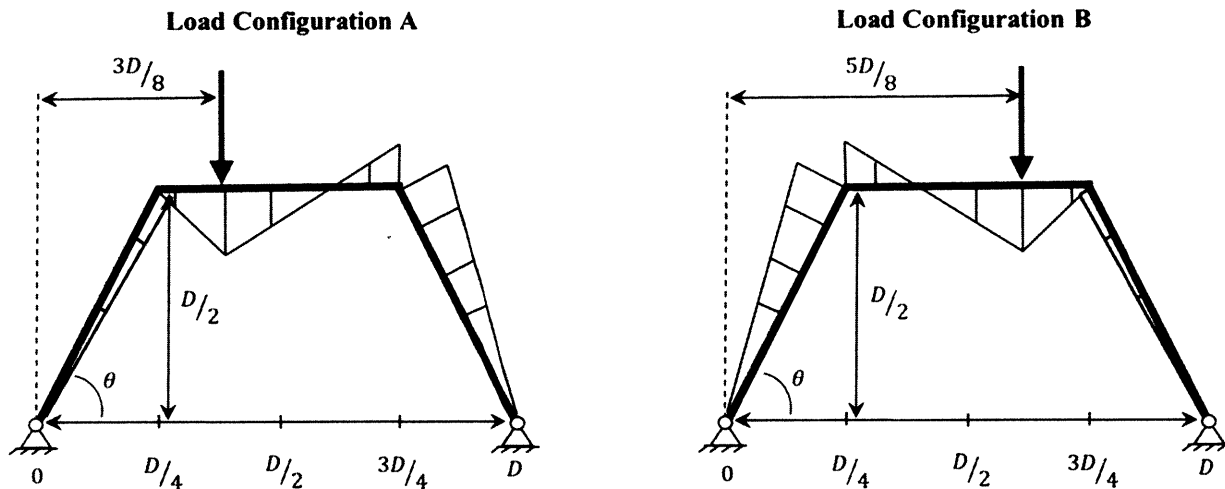**Load Configuration A**   **Load Configuration B**

Figure 2.1.

The sum of all possible bending moments that the frame experiences can readily be found through applying the principle of superposition and combining the moment envelopes of both loading scenarios, as shown on the left in Figure 2.2.
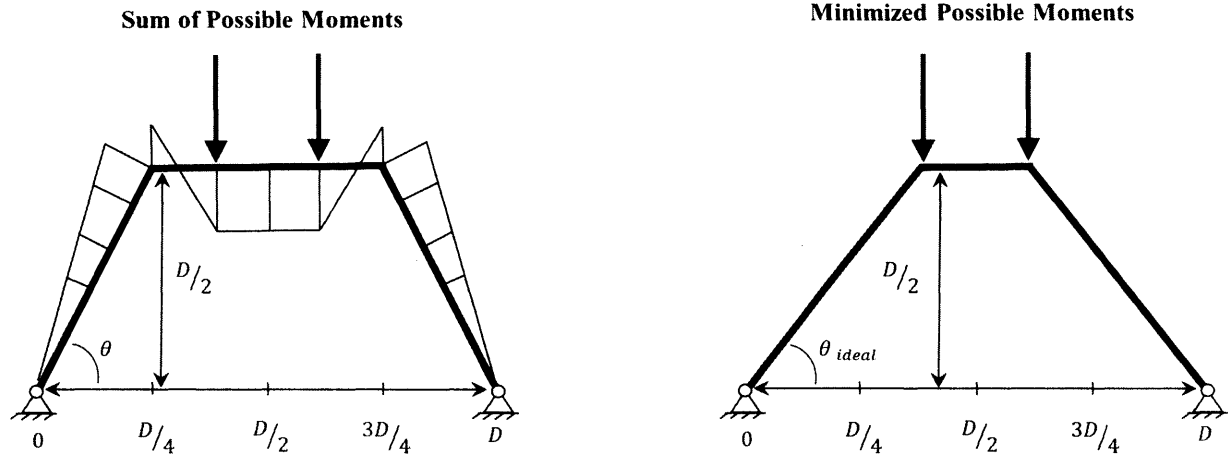
13

Sum of Possible Moments

Minimized Possible Moments

Figure 2.2.

The area of the moment envelope for the frame on the left expresses the bending moments that the frame could experience when subjected to the sum of all possible loads. Keeping all parameters of the frame geometry constant except for the depicted angle θ, a new frame defined by θ_{ideal} can be found that minimizes the moment envelope area when load configurations A and B are superimposed. This minimized aggregate moment value equals zero for the frame example on the right, as well as for any scenario in which a zero-moment structure geometry exists when all possible load configurations are superimposed, which is always the case for simply-connected networks, including arch-like structures. We will return to this observation later in the derivation. However, our problem description states that load configurations A and B will never occur simultaneously. We therefore seek to determine if the altered frame geometry as defined by θ_{ideal} is also the optimal shape for the individual load configurations when each load case has an equal probability of occurrence. Because the bending moment at any specific position $M(x)$ along the frame for an individual load configuration was not necessarily optimized by modifying the frame geometry, we begin the initial derivation by expressing the sum of all possible moments as a function of the frame geometry and optimizing for the summed moment distribution. The result will demonstrate that the frame defined by θ_{ideal} above is also moment-optimized for the summed individual load configurations A or B when applied separately. This theoretical framework will then be applied to arched structures; specifically, to demonstrate that the moment-optimized shape $y(x)$ for an arch subjected to a simple stochastic loading condition, meaning a fully random application of a point load P, is equal to the ideal arch shape when a horizontally-projected uniform distributed load is applied.

14

2.2 Moment Equation Assembly

Consider the same frame example subjected to load configuration A. While the height of the center member of the frame is held constant at $D/2$, the horizontal position of nodes A and B are determined by the variable b. Due to the indeterminacy of the frame, the magnitude of the horizontal reactions will be considered constant. This constant value is set to $\frac{2P}{3}$ for this derivation as it is within a range a reasonable possible horizontal reaction values. In future studies beyond the material presented in this thesis, the reaction value that minimizes strain energy should be used. To sum all possible experienced moments, the equations for the moments $m_{1-5}(x)$ throughout the frame must first be identified using the variable b as a parameter.

Load Configuration A
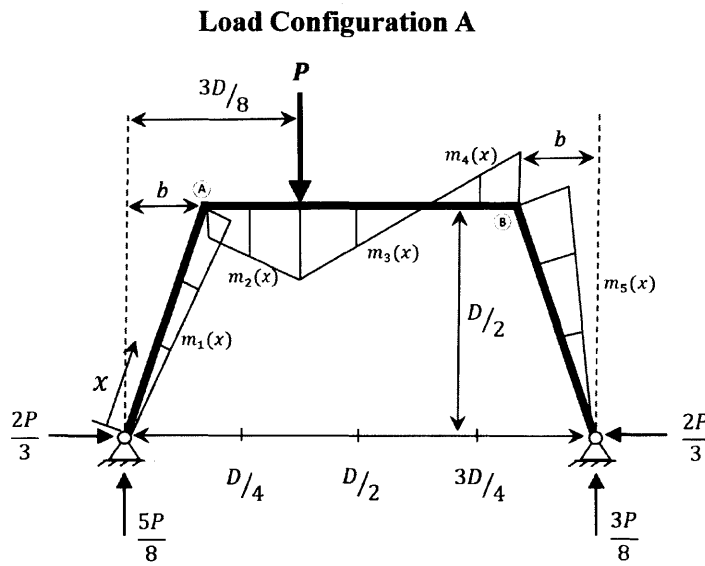
Figure 2.3.

The variable x defines the distance from the left support along the surface of the frame. Using the method of sections and summing the moments at sectioned intervals of distance x from the left support, the following equations are produced for $0 \leq b \leq \frac{3D}{8}$.

$$\sum m_x = 0$$

$$m_1(x) = \left(\frac{xP}{\sqrt{b^2 + \frac{D^2}{4}}} \right)\left(\frac{5b}{8} - \frac{D}{3} \right) \quad \text{for} \quad 0 < x < \sqrt{b^2 + \frac{D^2}{4}}$$

$$m_2(x) = -\frac{5P}{8}(x - b) - \frac{DP}{3} \quad \text{for} \quad 0 < x < \frac{3D}{8} - b$$

15

The equations $m_3(x)$ and $m_4(x)$ are equivalent but must each be integrated over different intervals when summing the moment envelopes, as the moment value changes from negative to positive. The projection of the equations $m_n(x)$ onto the frame surface are shown in figure 2.4 below.

$$m_3(x) = m_4(x) = P\left(D\left(\frac{11(D+4x)}{48(8b-5D)} - \frac{17}{16}\right) + \frac{23b}{8} + \frac{13x}{8}\right) \quad \text{for} \quad \frac{3D}{8} - b < x < (D - 2b)$$

$$m_5(x) = P\left(\frac{D}{3} - \frac{3b}{8}\right)\left(1 - \frac{x}{\sqrt{b^2 + \frac{D^2}{4}}}\right) \quad \text{for} \quad 0 < x < \sqrt{b^2 + \frac{D^2}{4}}$$

**Moment Envelope Projection onto Frame Surface
for Load Configuration A**
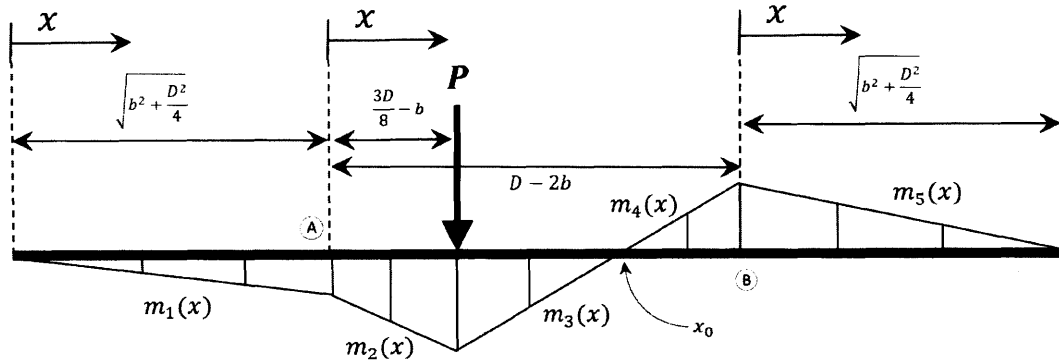
Figure 2.4.

To find the total area of the moment envelope for load configuration A, each equation $m_n(x)$ must be integrated over its respective interval. The absolute values of each area $A_n(b)$ can then be summed into one overall expression defining the moment envelope in terms of the variable b.

$$A_1(b) = \int_0^{\sqrt{b^2 + \frac{D^2}{4}}} m_1(x)\, dx = \frac{P(15b - 8D)}{96}\sqrt{4b^2 + D^2}$$

$$A_2(b) = \int_0^{\frac{3D}{8} - b} m_2(x)\, dx = \frac{-P(2880b^2 - 2464bD + 519D^2)}{3072}$$

16

To determine the integration interval for equations $m_3(x)$ and $m_4(x)$, the position x_0 at which the moment switches signs must first be identified:

$$m_{3,4}(x_0) = 0 \qquad \Rightarrow \qquad x_0 = \frac{-552b^2 + 549bD - 133D^2}{312b - 173D}$$

$$A_3(b) = \int_{\frac{3D}{8}-b}^{x_0} m_3(x)\, dx = \frac{-P(240b - 109D)(6912b^2 - 4840bD + 545D^2)}{3072(312b - 173D)}$$

$$A_4(b) = \int_{x_0}^{D-2b} m_4(x)\, dx = \frac{P(9b - 8D)(146016b^2 - 221052bD + 81120D^2)}{97344(312b - 173D)}$$

$$A_5(b) = \int_0^{\sqrt{b^2+\frac{D^2}{4}}} m_5(x)\, dx = \frac{P(8D - 9b)}{96}\sqrt{4b^2 + D^2}$$

The absolute values of these areas $A_{1-5}(b)$ are summed to produce one equation $A_{total}(b)$. The moment envelope for load configuration B must also be considered. Symmetry allows for the sum of the moments from load configuration A to simply be doubled to produce $A_{total}(b)$.

$$A_{total}(b) = 2\sum_{i=1}^{n} |A_n(b)|$$

Solving for the exact solution for $A_{total}(b)$ by hand would require lengthy, arduous calculations. The equation however was mathematically programmed to produce the plot below (Wolfram).
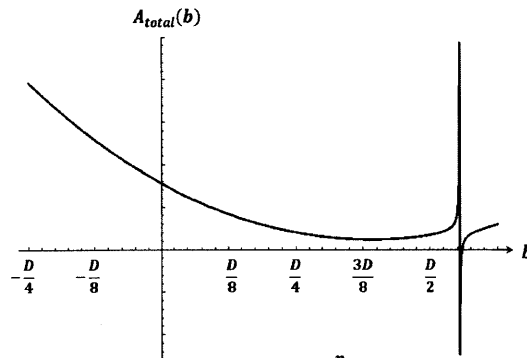

Figure 2.5. $A_{total}(b) = 2\sum_{i=1}^{n} |A_n(b)|$

17

The complex polynomial expresses the summed moments experienced from both loads as a function of b. $A_{total}(b)$ is positive over the interval of physically possible b values from 0 to $\frac{3D}{8}$, as expected.

2.3 Deriving the Exact Solution for b

Setting the partial derivative $\frac{\partial}{\partial b}$ of the expression $A_{total}(b)$ equal to zero and solving for b will produce the value for b at which the frame experiences a minimum for potential moments. To aid in simplifying this calculation, the partial derivatives of each $A_n(b)$ are first determined, then summed and equated to zero.

$$\frac{\partial}{\partial b}A_1(b) = \frac{P(120b^2 - 32bD + 15D^2)}{96\sqrt{4b^2 + D^2}}$$

$$\frac{\partial}{\partial b}A_2(b) = -\frac{15bP}{8} + \frac{77DP}{96}$$

$$\frac{\partial}{\partial b}A_3(b) = \frac{P(-8087040b^3 + 11394072b^2D - 5176506bD^2 + 745015D^3)}{24(312b - 173D)^2}$$

$$\frac{\partial}{\partial b}A_4(b) = \frac{P(9b - 8D)(22464b^2 - 25704bD + 7081D^2)}{24(312b - 173D)^2}$$

$$\frac{\partial}{\partial b}A_5(b) = \frac{-P(72b^2 - 32bD + 9D^2)}{96\sqrt{4b^2 + D^2}}$$

$$\frac{\partial}{\partial b}A_{total}(b) = 2\frac{\partial}{\partial b}\sum_{i=1}^{5}|A_n(b)| = 0$$

$$\frac{\partial}{\partial b}A_{total}(b) = \frac{24b^2 - 8bD + 3D^2}{12\sqrt{4b^2 + D^2}} - \frac{15b}{8} + \frac{77D}{96} + \frac{\alpha}{24(312b - 173D)^2} = 0$$

where $\alpha = -7884864b^3 + 10983024b^2D - 4907124bD^2 + 688367D^3$

$$\frac{\partial}{\partial b}A_{total}(b) = 0 \text{ reduces to:}$$

$$12\sqrt{4b^2 + D^2} = \frac{56070144b^4 - 80870400b^3D + 44974656b^2D^2 - 13518912bD^3 + 2154888D^4}{12265344b^3 - 17714736b^2D + 8332005bD^2 - \frac{1}{4}(5058001D^3)}$$

18

The approximate solutions to this fourth degree polynomial are as follows:

$$b_1 \approx 0.378498D$$

$$b_2 \approx 0.552009D$$

$$b_3 \approx 0.552650D$$

$$b_4 \approx 0.556483D$$

Referencing Figure 2.5, the solutions b_{3-4} identify the locations of asymptotes of the expression $A_{total}(b)$ are also outside the range of physically possible values for b. Our solution therefore is b_1.

$$b \approx 0.378498D \approx \frac{3D}{8}$$

ANS.

The exact value of b is approximately three-thousandths away from the distance $\frac{3D}{8}$ at which the point loads from load configurations A or B are applied. This is due to the chosen constant value for the horizontal reaction, which will mildly influence the moments experienced at the frame's fixed joints and, therefore, the optimal geometry.

Optimal Shape for Load Configurations A or B

Figure 2.6.

19
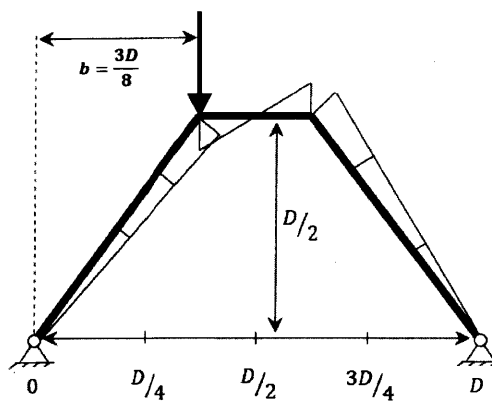
We now seek to determine the optimal shape for the frame when both loads are applied simultaneously and compare with this derived solution.

2.4 Optimal Frame Geometry for the Superimposed Load Case

Having derived an optimal value for b by minimizing the sum of the absolute values of all possible moment envelopes, we now seek to determine the optimal value for b considering load configurations A and B are applied together. Because we already know the moment equations $m_n(x)$ along the length of the frame for the individual load configurations, we will simply evaluate the equations at their maximum locations and use the principle of superposition.

$$m_1\left(\sqrt{b^2 + \frac{D^2}{4}}\right) = P\left(\frac{5b}{8} - \frac{D}{3}\right)$$

$$m_2\left(\frac{3D}{8} - b\right) = -\frac{5P}{8}\left(\frac{3D}{8} - 2b\right) - \frac{DP}{3}$$

$$m_5(0) = P\left(\frac{D}{3} - \frac{3b}{8}\right)$$

Because we know that an optimal geometry will experience zero bending moments, we sum the individual maximum moments from each frame element and from each load case, set that value equal to zero by using the principle of superposition, and solve for b.

$$\frac{5b}{8} - \frac{D}{3} - \frac{5}{8}\left(\frac{3D}{8} - 2b\right) - \frac{D}{3} + \frac{D}{3} - \frac{3b}{8} = 0$$

$$\frac{3b}{2} = \frac{D}{3} + \frac{15D}{64}$$

$$b = \frac{109D}{288} \approx 0.3784D \approx \frac{3D}{8}$$

<div align="right">**ANS.**</div>

We see that the optimal position of the nodes for the zero-moment frame geometry align with the superimposed load's lines of action, which were at $x = \frac{3D}{8}$ for load A and $x = \frac{5D}{8}$ for load B. Once again, the slight difference in b values is due to the chosen horizontal reaction value. This

moment-optimized value of $b = \frac{3D}{8}$ that defines the frame geometry for the superimposed load case where all moments equal zero is the same value as for the possible load configurations applied individually, as shown in Figure 2.7 below.
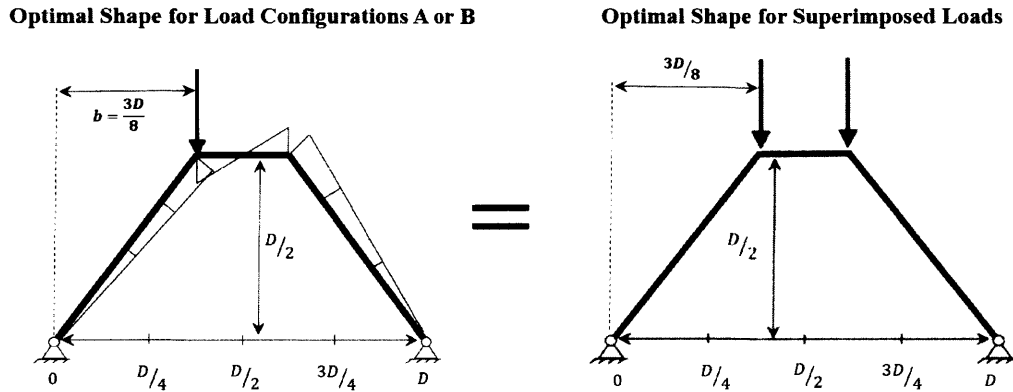
Optimal Shape for Load Configurations A or B   Optimal Shape for Superimposed Loads

Figure 2.7.

This result suggests that the moment-optimized shape for a structure with a certain set of equally possible loading conditions will be equal to the zero-moment shape when all loads are simultaneously applied. We will refer back to this observation when constructing a general theorem. The result also emphasizes a highly useful application of the principle of superposition by demonstrating that for a set of possible load configurations, where one load from the set is fully randomly applied, the optimal geometry may be found by summing the moment distributions from each possible load configuration and equating the summation to the moment distribution when all loads are applied at once, as discussed in Section 2.1. Recognizing that the optimal shape when all loads are simultaneously applied will experience zero moment, the relationship may be mathematically expressed as follows:

$$\sum_{i=1}^{N} M_N = 0 \qquad \text{for optimal geometry}$$

where N = individual load configuration
M_N = moment envelope for configuration N

As was demonstrated in the preceding derivations, the application of Equation 2.1 is much less computationally arduous than summing the absolute values for all possible moment distributions. This specific application of superposition will therefore be used to assess the theoretical

generalization of the frame derivation to arched structures subjected to a fully random application of a point load P along the length of the arch.

3. The Simple Stochastic Load Case

3.1 Generalization

We now return to the question of the optimal arch shape $y(x)$ subjected to a simple stochastic loading condition, meaning a fully random application of a point load P, and apply the relationships identified from the previous frame example. Consider the following arch of unknown shape subjected to the stochastic point load P and defined by the assumptions established in Table 1.1.
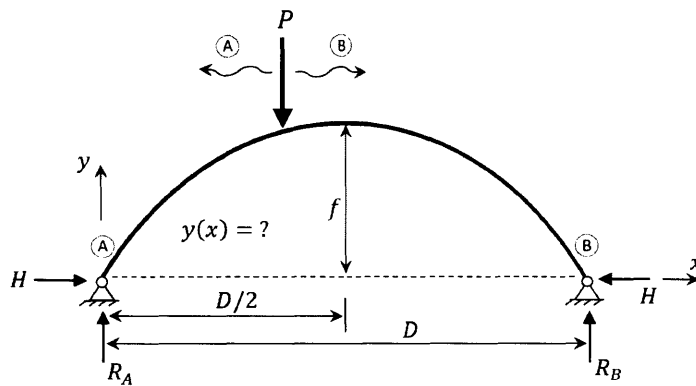

Figure 3.1.

We seek to determine the optimized shape $y(x)$ for the arch such that all possible bending moments are minimized. Recall that the optimal frame geometry for two possible loading scenarios with an equal probability of occurrence is equal to the ideal geometry when both possible loads are superimposed. Expanding on this relationship by introducing three possible load cases where the points of application are all at equally horizontally-segmented distances $\frac{D}{4}$, the below ideal frame geometry derived from the superposition of these loads could be found. **Figure 3.2.**

r.

**Load Configurations A, B and C**   **Superimposed Loads**
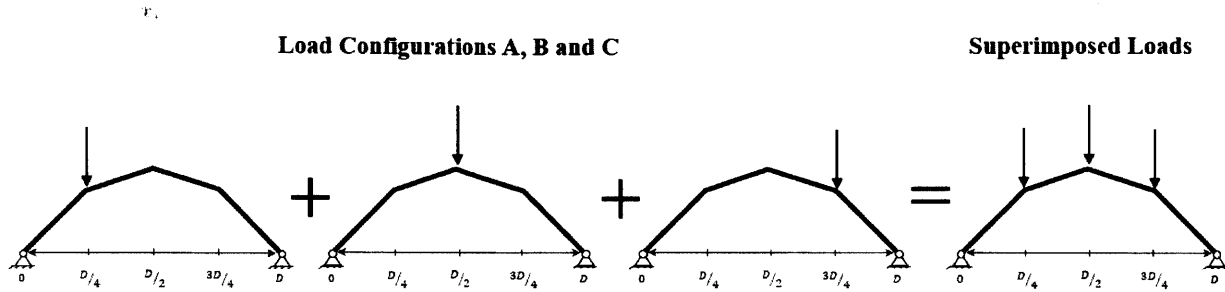
If instead we considered a set of four possible load cases where the points of application were again equally horizontally-segmented distances $\frac{D}{5}$, we could again derive the optimal frame shape through the relationship established in Chapter 2. This optimal frame would have five individual frame elements and would begin to appear funicular in shape. The arch in Figure 3.1 is subjected to a single point load P with a fully random probability of occurrence at any location along its surface. Because we know that the moment-optimized shape for a structure with a certain set of equally possible loading conditions will be equal to the zero-moment shape when all loads are simultaneously applied, the simple stochastic load case is the theoretical equivalent of an infinite number of possible point loads where the points of application are equally horizontally-segmented distances of infinitesimal length dx. The superimposed load case could therefore be found by integrating the stochastic load P over the range of possible load locations.

$$\int_0^D P \, dx = PD \quad \text{uniform distributed load}$$

Therefore, the optimum shape for an arch $y(x)$ subjected to a simple stochastic load is equal to the ideal solution $y(x)$ for an arch under a horizontally projected uniform distributed load.
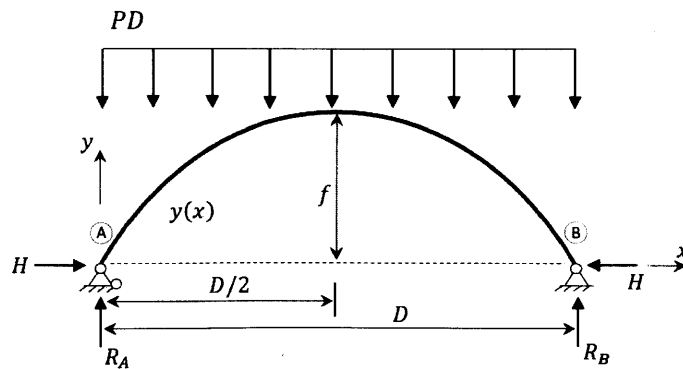
Figure 3.3. Superimposed simple stochastic load case.

25

The funicular solution for an ideal arch subjected to a horizontally projected uniform distributed load is shown below. This equation is derived in *Appendix A*.

$$y\,(x) = \frac{4xf}{D^2}(D - x)$$

We will now consider the superposition load case, which is the horizontal distributed load, in greater detail in preparation for generalizing to a variable stochastic load case.

3.2 Equivalent Load Construction using Superposition

Similar to the derivation in section 2.4, we now sum all possible maximum bending moments and equate the summation to zero, as the optimal shape for the superimposed load case will experience zero bending moment. We first need an expression M_{max} for each individual random application of the stochastic load. We know that the maximum moment for an optimized arch subjected to a point load will occur at the location of the point load. Therefore, the moment $M(x)$ will refer to the maximum moment at x, which is also the position of the point load. For the arch in Figure 3.1, moment equilibrium requires that the left vertical reaction equal $\frac{(D-x)}{D}P$ and the right reaction equal $\frac{x}{D}P$. We now consider an arch segment of length dx at horizontal distance x from node A. The horizontal reaction H at nodes A and B will be used as scaling factors once the equation of the arch has been determined. The vertical reactions are equivalent to the vertical components of the arch's internal forces acting directly to the left and right of the stochastic load's point of application. Therefore, we examine the forces occurring at a length $\pm\frac{dx}{2}$ from x.
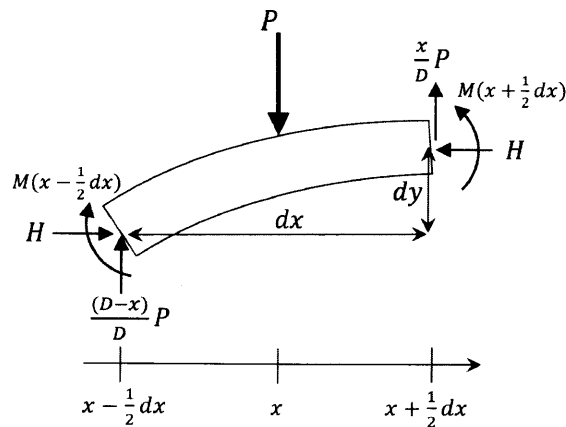

Figure 3.4.

26

The magnitude of the horizontal component of the arch's internal forces is equivalent to the horizontal reaction H at the supports and remains constant throughout the arch. Applying static equilibrium produces the following equation:

$$\sum M_{x+\frac{1}{2}dx} = 0$$

$$-M\left(x + \frac{1}{2}dx\right) + \left(\frac{D-x}{D}\right)Pdx - Hdy - P\left(\frac{dx}{2}\right) + M\left(x - \frac{1}{2}dx\right) = 0$$

Rearranging terms to isolate the moment function and dividing all components by dx gives:

$$\frac{M(x + \frac{1}{2}dx) - M(x - \frac{1}{2}dx)}{dx} = \left(\frac{D-x}{D}\right)P - H\frac{dy}{dx} - \frac{P}{2}$$

Recognizing the terms on the left as an approximation of the definition of a derivative as given by $\lim_{a \to 0} \frac{f(x+a)-f(x)}{a} = f'(x)$, the right side of the equation may be equated to $\frac{dM(x)}{dx}$. Integrating this expression with respect to x produces a function of the distribution of maximum moments.

$$M_{max}(x) = \int \left(\left(\frac{D-x}{D}\right)P - H\frac{dy}{dx} - \frac{P}{2}\right)dx$$

$$M_{max}(x) = \frac{Px}{2} - \frac{Px^2}{2D} - Hy(x)$$

Because this expression both varies as a function of x and is always the maximum value for the individual load P applied at x, the equation represents a moment envelope of maximum moments for every possible load scenario. Using the principle of superposition, we then equate this value to zero to determine the optimum shape $y(x)$.

$$\frac{Px}{2} - \frac{Px^2}{2D} - Hy(x)$$

$$y(x) = \frac{Px}{2HD}(D - x)$$

$$y\left(\frac{D}{2}\right) = f \quad \Rightarrow \quad H = \frac{PD}{8f}$$

$$\Rightarrow \quad y(x) = \frac{4xf}{D^2}(D - x)$$

ANS.

27

This process is equivalent to optimizing the arch shape under a horizontally distributed uniform projected load. We now seek to determine whether this relationship applies to stochastic loading scenarios where the likelihood of the load's occurrence is not fully random but instead varies across a certain length.

4. The Variable Stochastic Load Case

In section 3.1 we proved that the optimal shape $y(x)$ for a fully random stochastic load P is equal to the zero-moment solution for an arch subjected to a horizontally uniform distributed load. We now seek to generalize this equality for stochastic loading conditions where the location of the load P is not fully random but instead governed by a probability density function $f(x)$. Consider again the theoretical expansion of the initial frame derivation, where the moment-optimized shape for a structure with a certain set of equally possible loading conditions will be equal to the zero-moment shape when all loads are simultaneously applied. For a variable stochastic load case, the set of possible loading scenarios are given a weighted possibility of occurrence. The following derivation assumes that the moment-optimized shape for such a variable stochastic loading scenario will be equal to the zero-moment geometry under the superimposed set of loads when the magnitudes of the superimposed loads are weighted averages of their corresponding individual load's likelihood of occurrence. The frequent use of weighted averages for analyzing the probabilities of load occurrence in structural topology optimization combined with the relationship derived in the initial frame example justify this assumption. This assumption is further corroborated with the programmed moment-minimizing software models discussed in Chapter 6. A simple frame example depicts the assumption below, where the likelihood of occurrence for load configuration A is twice that of load configuration B.
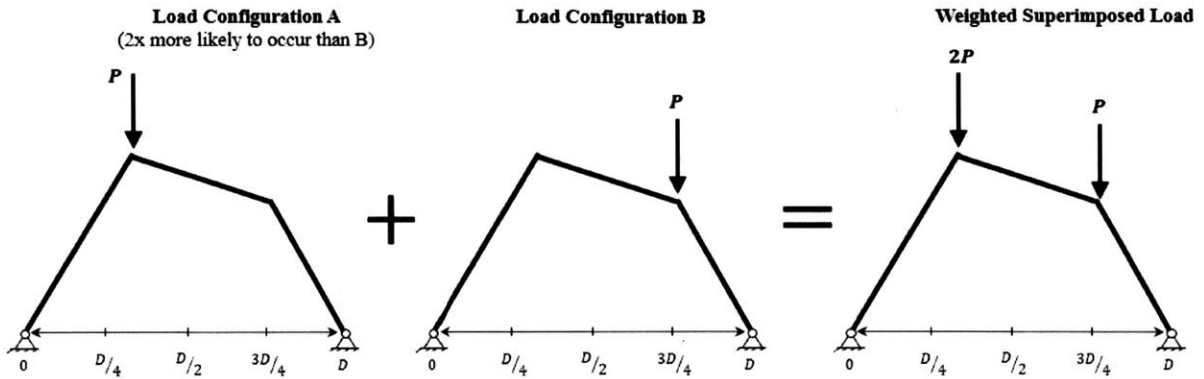
Figure 4.1.

4.1 The Probability Density Function

A probability density function must be positive over the predetermined length of interest L from a to b, as well as have an area equal in magnitude to that length L. To define the likelihood of the location of the load P, we choose a probability density function that is symmetric over length L as well as continuously differentiable such that a comparison analogous to the equality found in the previous derivation may be evaluated. Consider the below probability density function $f(x)$, where D represents the distance over the support from a to b. Integrating over the support yields:

$$f(x) = \frac{-6x^2}{D^2} + \frac{6x}{D} \quad \Rightarrow \quad \int_{x=0}^{x=D} f(x)dx = \frac{-2D^3}{D^2} + \frac{3D^2}{D} = D$$
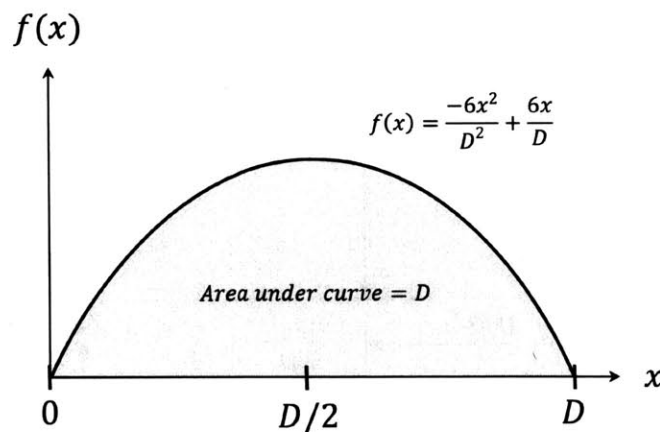

Figure 4.2.

29

The area under the curve D is analogous to the probability of occurrence of a load P at some distance x from 0 to D. Assuming that the stochastic load must occur, the area D represents a complete chance of occurrence somewhere along the surface of the arch. Note that this area could have been any value; the specific probability density function $f(x)$ was chosen in part to simplify calculations and to clarify the relationship between the stochastic loads and the superimposed loads.

4.2 Equivalent Load Construction using Superposition

We seek to construct the equivalent uniform load for the variable stochastic load case using superposition and the relationship defined from the initial frame derivation in Section 3.2. As defined above, the probability density function $f(x)$ states that a load P is more likely to occur towards the center of a given structure. Consider the following arch of unknown shape $y(x)$ subjected to the variable stochastic point load P.
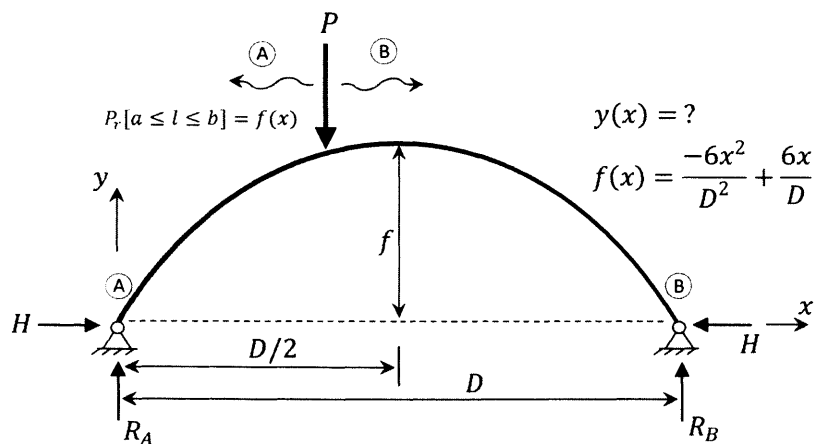

$$P_r[a \le l \le b] = f(x)$$

$$y(x) = ?$$

$$f(x) = \frac{-6x^2}{D^2} + \frac{6x}{D}$$
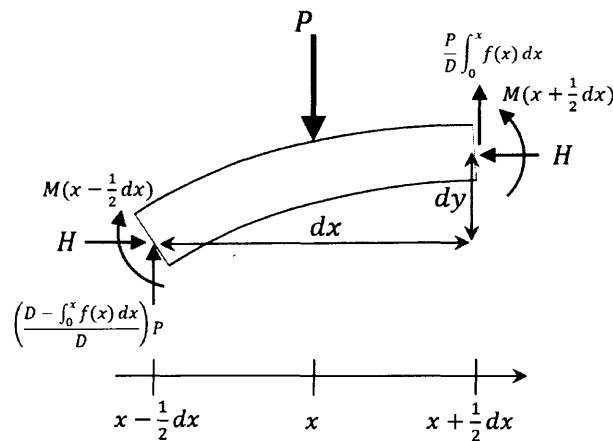
Figure 4.3

Once again we seek to determine the optimized shape $y(x)$ for the arch such that the bending moment $M(x)$ is minimized. Whereas previously the variable x determined the location of the load P, that distance now characterizes the probability of occurrence of P at x by defining it as the integral of the probability density function $f(x)$ from 0 to x. The *stochastic reactions* resulting from this substitution would therefore not be the true reactions but instead represent the probability that $R_A = \frac{P(D-x)}{D}$, for example, will occur given the likelihood that P occurs is governed by $f(x)$. Applying static equilibrium, these stochastic reactions are determined:

$$\sum M_B = 0 \quad \Rightarrow \quad D * R_A - \left(D - \int_0^x f(x)\,dx\right) * P = 0 \quad \Rightarrow \quad R_A = \left(\frac{D - \int_0^x f(x)\,dx}{D}\right)P$$

$$\sum F_y = 0 \quad \Rightarrow \quad R_B = P - R_A \quad \Rightarrow \quad R_B = \frac{P}{D}\int_0^x f(x)\,dx$$

Once again, the horizontal reaction H at nodes A and B will be used as a scaling factor for $y(x)$.

We again consider an arch segment of length dx at horizontal distance x from node A and examine the forces occurring at a lengths $\pm\frac{dx}{2}$ from x. The previously determined stochastic reactions are equivalent to the vertical components of the arch's internal forces acting on the faces of the arch segment.

Figure 4.4.

Applying static equilibrium produces the following equations:

31

$$\sum M_{x+\frac{1}{2}dx} = 0$$

$$-M\left(x + \frac{1}{2}dx\right) + \left(\frac{D - \int_0^x f(x)\,dx}{D}\right)Pdx - Hdy - P\left(\frac{dx}{2}\right) + M\left(x - \frac{1}{2}dx\right) = 0$$

Rearranging terms to isolate the moment function and dividing all components by dx gives:

$$\frac{M(x + \frac{1}{2}dx) - M(x - \frac{1}{2}dx)}{dx} = \left(\frac{D - \int_0^x f(x)\,dx}{D}\right)P - H\frac{dy}{dx} - \frac{P}{2}$$

We again equate the left side of the above equation to $\frac{dM(x)}{dx}$ and recall that the maximum bending moment M_{max} will occur at the location x of the stochastic load, and that it represents a moment envelope of maximum moment values for all possible loads, allowing $M(x) = 0$.

Integrating $\frac{dM(x)}{dx}$ and equating that expression $M(x)$ to zero produces the following equations:

$$\frac{dM(x)}{dx} = \left(\frac{D - \int_0^x f(x)\,dx}{D}\right)P - H\frac{dy}{dx} - \frac{P}{2} = 0$$
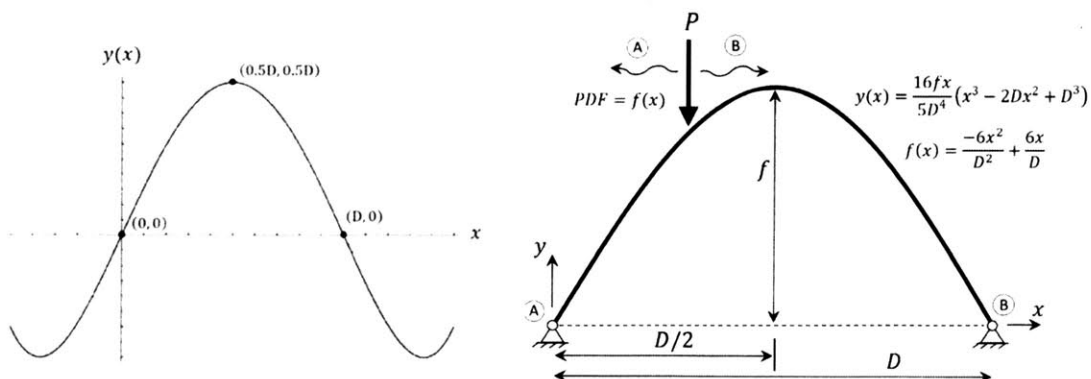
$$\int_0^x f(x)\,dx = \frac{-2x^3}{D^2} + \frac{3x^2}{D}$$

$$y(x) = \frac{P}{H}\left(\frac{-x^4}{2D^3} + \frac{x^3}{D^2} - \frac{1}{2}x\right)$$

$$y\left(\frac{D}{2}\right) = f \quad \Rightarrow \quad H = \frac{-5PD}{32f}$$

$$\Rightarrow \quad y(x) = \frac{16fx}{5D^4}(x^3 - 2Dx^2 + D^3)$$

<div align="right">ANS.</div>

This equation represents the moment-optimized arch shape for which the weighted stochastic

loads are superimposed and is graphed below. As expected, the arch appears semi-linear close to the supports where the load concentration is relatively low.

Figure 4.5.

The funicular solution for an ideal arch subjected to a non-uniform distributed load $u(x)$ where $u(x)$ is equal to the probability density function $f(x)$ is shown below. This equation is derived in *Appendix B* and is equal to the optimal arch shape for the stochastic load described above.

$$y(x) = \frac{16fx}{5D^4}(x^3 - 2Dx^2 + D^3)$$

We now summarize the derivation presented in Section 3.2 and its associated applications into a generalized conjecture for stochastic loading.

5. Stochastic Loading for Arches

The initial frame derivation in section 3.1 demonstrated that the moment-optimized structural topology when subjected to a certain set of equally possible loading configurations must be identical to the zero-moment solution when all possible loads are superimposed. From this derivation the optimal form for an arch subjected to a fully random application of a point load was found to equal the ideal arch shape for a horizontally projected uniform distributed load. Further extensions then equated the probability density function governing the likelihood of occurrence of a load to a weighted superposition of all possible loads for the optimal geometry. In each of the above cases, the likelihood of occurrence directly describes the nature of the superimposed load case: uniformly distributed for a fully random point load, weighted average for point loads at fixed locations with dissimilar probabilities of occurrence, and non-uniformly distributed for varying likelihoods of occurrence over an interval. Generalizing the results of these derivations, a conjecture for stochastic loading may be stated as follows: *the equation* $y_1(x)$ *for an arch, having been optimized to experience a minimum summation of the absolute value of all possible bending moment envelopes while subjected to a stochastic point load P, the point of application x for which being determined by a probability density function* $f(x)$ *over the support from a to b, is equal to the zero-moment solution* $y_2(x)$ *for an arch subjected to a distributed load* $u(x)$ *on the interval from a to b when* $f(x) = u(x)$. For discontinuous intervals, where the probability of occurrence for a stochastic load is zero, the equivalent superimposed load would also be zero; the optimal shape on that interval would be linear. Therefore, the generalized conjecture above also includes frame geometries and arch-frame topology combinations. A general visual representation of the theorem is depicted below.
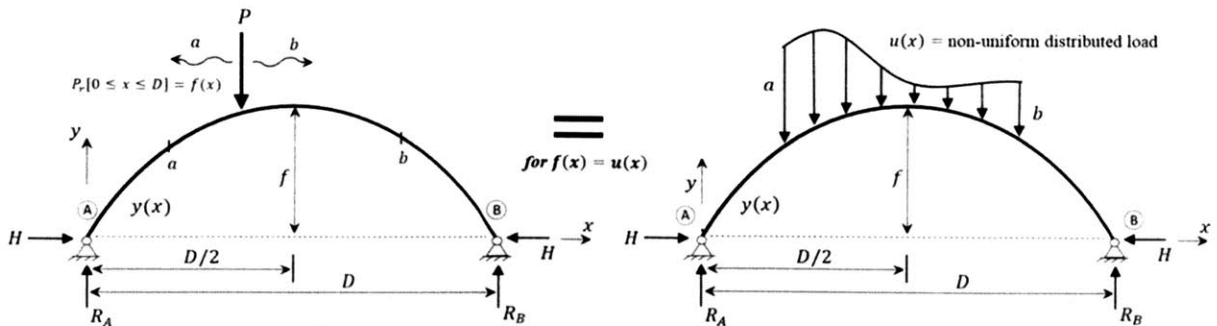

Figure 5.1. Stochastic Loading for Arches Conjecture.

Two corollaries of the conjecture are included below.

1. The magnitude of the stochastic point load P or of $u(x)$ at any given x will not affect the resulting shape $y(x)$ of the arch.

2. Doubly-integrating the probability density function for a stochastic point load P will produce the optimal shape: $\iint f(x) = y(x)$.

We now seek to further explore the above relationships using numerical methods by programming various stochastic loading scenarios into structural analysis software models and comparing the resulting arch typologies.

6. Geometrical Form-Finding

6.1 General Model Construction

Rhino 3D CAD software aided by the Grasshopper plugin was used to construct the arch models. The objective is to test the mathematical relationships previously defined using numerical methods by programming the various loading scenarios into Rhino 3D CAD software models and comparing the resulting arch typologies. The primary model is an arch-like frame segmented into 20 equidistant nodes along its length and containing the possibility for a unit point load to be applied at every node. A line of best fit applied to five points of heights h_n and measured at five equidistant intervals between the pinned supports defines the shape $y(x)$ of the arch, making the heights h_{1-5} the primary variables. The large number of equally spaced nodes causes the many point loads to replicate a distributed load if all applied at once, or allows for point loads to be applied individually and sporadically in any chosen combination of nodes from one to twenty.
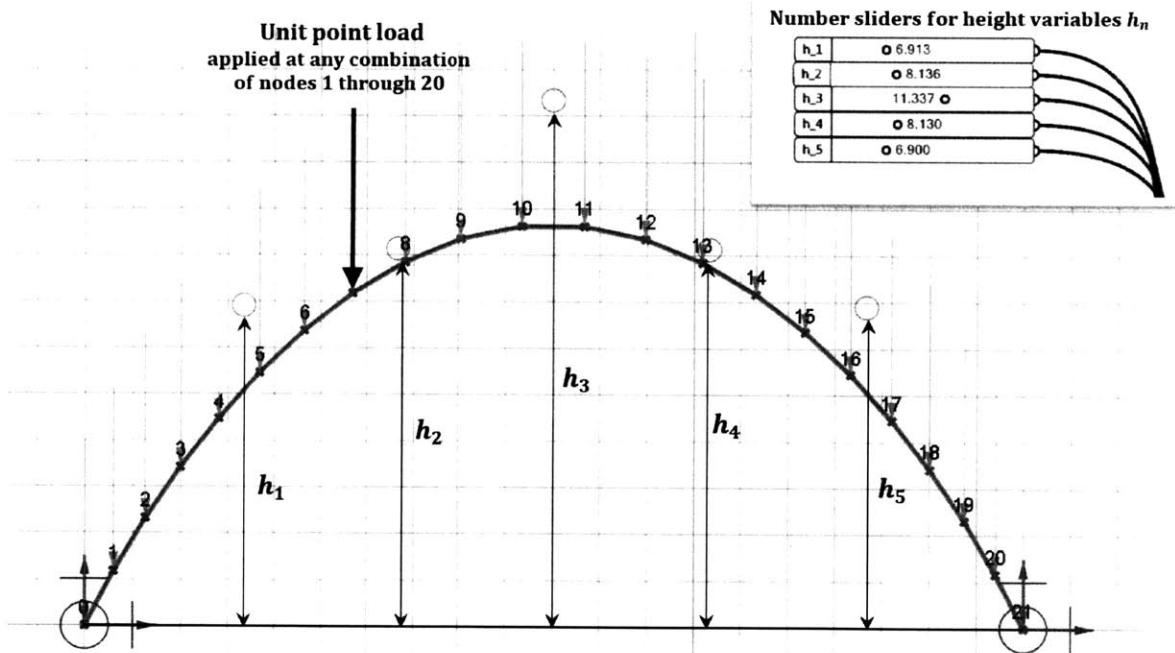

Figure 6.1. Visual for model definition.

When a certain load combination is applied, the Grasshopper program analyzes the structure for the geometry defined by the heights h_n and outputs the maximum bending moment. The program then loops back and incrementally changes the parameter h_n using a global, evolutionary approximation algorithm, comparing the new maximum bending moment value with the previous value and adopting the new geometry if the bending moment has decreased. Iterating this process through thousands of combinations of h_n, the program terminates when a minimum possible bending moment has been found; the resulting geometry is the optimal arch for the given set of randomly chosen load combinations when considering the maximum bending moment experienced. This procedure is different from the frame derivation in section 3.2 in that it only considers the possible maximum bending moments, as opposed to the possible moment envelopes. The following results therefore serve as an extension to the stochastic loading conjecture previously stated. Additionally, optimizing for maximum bending moments aids in the design of structures with certain experienced moment and deflection criteria, as will be discussed in the case study.

## 6.2 The Simple Stochastic Load Case

First we seek to validate the results of the original derivation for a fully random point load. Twenty identical arches as described above are programmed into the Grasshopper file, each with a unit point load located at a different node, but each governed by the same five height parameters h_{1-5}. The program analyzes and compares the maximum bending moment in each possible load case independently, outputs a minimum value for the maximum moments of all twenty arches, and adjusts h_n. Every arch model responds to the geometry adjustments regardless of which model produced the smallest maximum bending moment for that iteration. The final shape of the arch is then compared to a model where all twenty nodes experience unit point loads simultaneously to approximate a uniform distributed load. The final shapes of both trials are shown below.

Figure 6.2.

Left arch: stochastic load
Right arch: "uniform" load
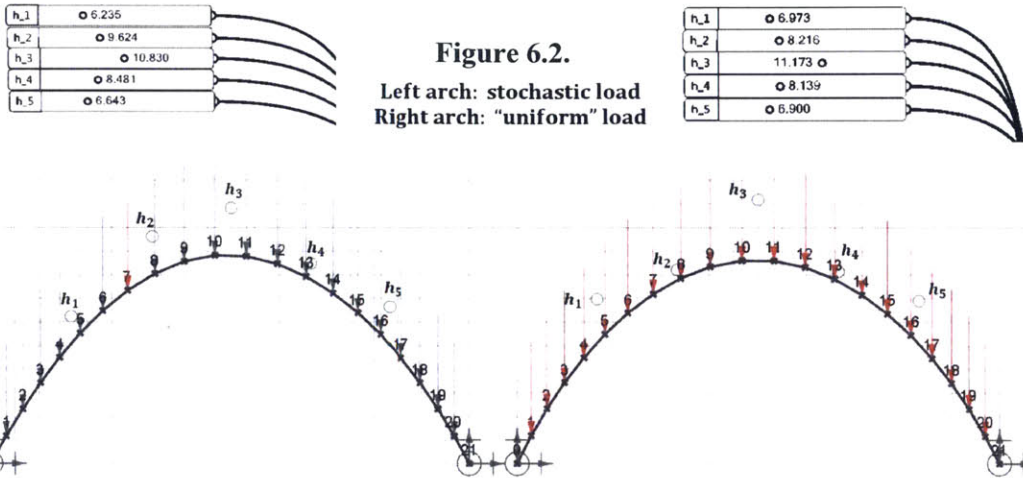
The final moment-minimized shapes for both loading scenarios are essentially identical, as predicted by the theorem. The h_{1-5} parameters for the arches do not arrive at the same numerical values due to the different responses of each structure's internal forces, but the final solutions $y(x)$ still converge to the same shape. The solution $y(x)$ is not a true parabola as the distance between nodes are equal segments of the arch length, not equidistant in the horizontal direction. However, the resulting shapes being equal confirms that the moment-optimized shape for a random point load is equal to that of a uniform distributed load as predicted by the theorem.
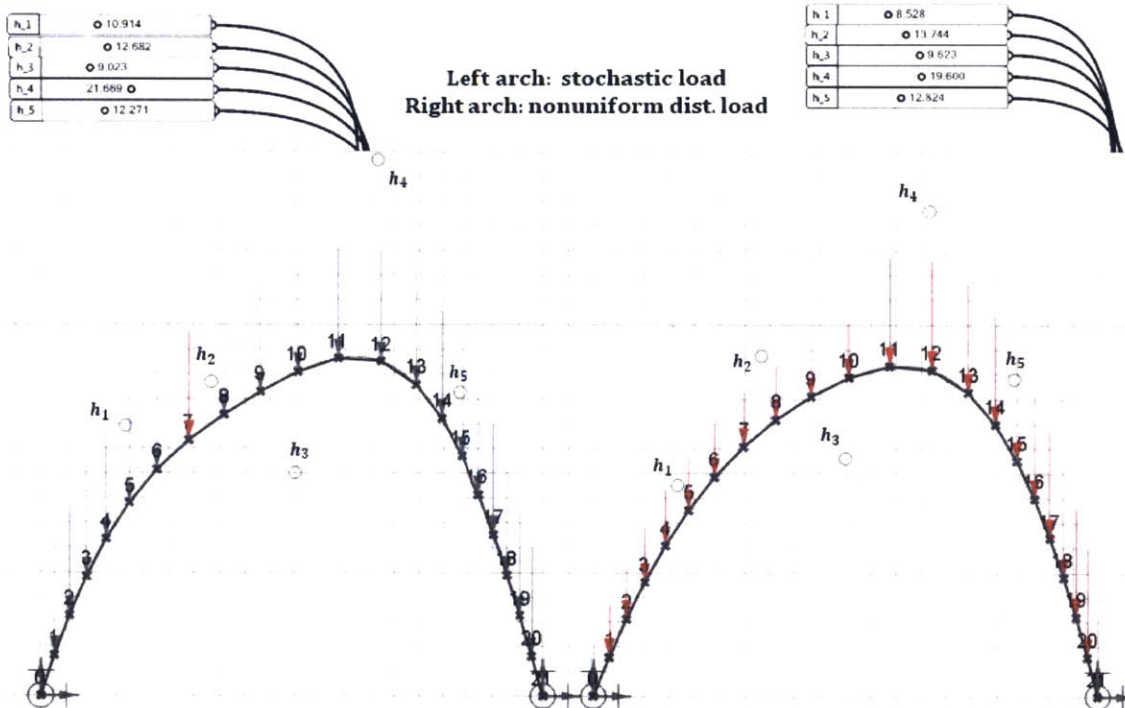
6.3 The Variable Stochastic Load Case

We now seek to validate the results from the derivation for a random point load whose probability of occurrence is governed by a probability density function $f(x)$. We choose a probability density function that describes a stochastic load condition where the likelihood of occurrence for a point load on the right half of an arch is double that of the left side of the arch, but constant across each respective half. Refer to the diagram below:

$$w = f(x) = \begin{array}{l} 2/3, 0 < x < D/2 \\ 4/3, D/2 < x < D \end{array}$$
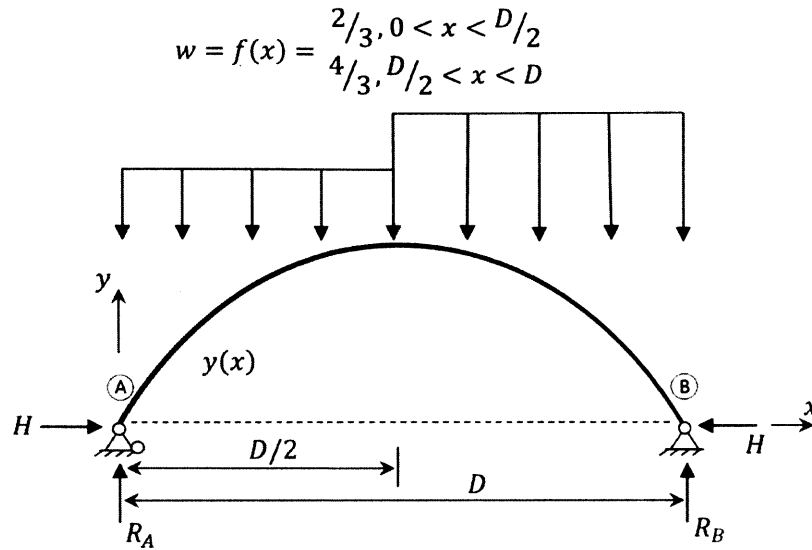
Figure 6.3. Probability density function.

Using a similar form-finding operation as before, a model with all point loads applied to each node simultaneously is compared to that of the randomly applied point loads.

The magnitudes of the point loads on the right half of the arches from both models are double that of the left side loads. The stochastically loaded arch considers an increased magnitude for a given point load as equivalent to an increased likelihood of occurrence at for the load at the associated node, similar to the reasoning in the derivation. The results are depicted below.

Figure 6.4. Demonstration of equivalence for the optimal arch shapes subjected to a variable stochastic load and non-uniform load.

As expected, the optimal arch shape for both scenarios are almost identical. Because a different probability density function $f(x)$ was used in the derivation in Chapter 4 than for this model, with the same results, we can safely assume that the conjecture holds true for any probability density function; that is, the moment-optimized arch shape for a distributed load $u(x)$ or for a point load randomly applied according to a probability density function $f(x)$ will be equal when $u(x) = f(x)$.

6.4 Varying the Interval

We now seek to determine if the above relationships hold true when also applied to load scenarios where the stochastic load can be applied only over a certain interval a to b instead of over the entire surface of the arched structure. The zero-moment solution for a structure over an interval where no load is applied is linear. Therefore, for the solution $y(x)$ for an arch shape over which a distributed load is only partially applied, we can reasonably expect a linear shape combined with a funicular shape for the sections where loads do not exist and where the arch is loaded, respectively.

Figure 6.5 below shows the results from the form-finding program when both the simple stochastic load and uniform distributed load are applied over an interval a to b at the center of the arch.
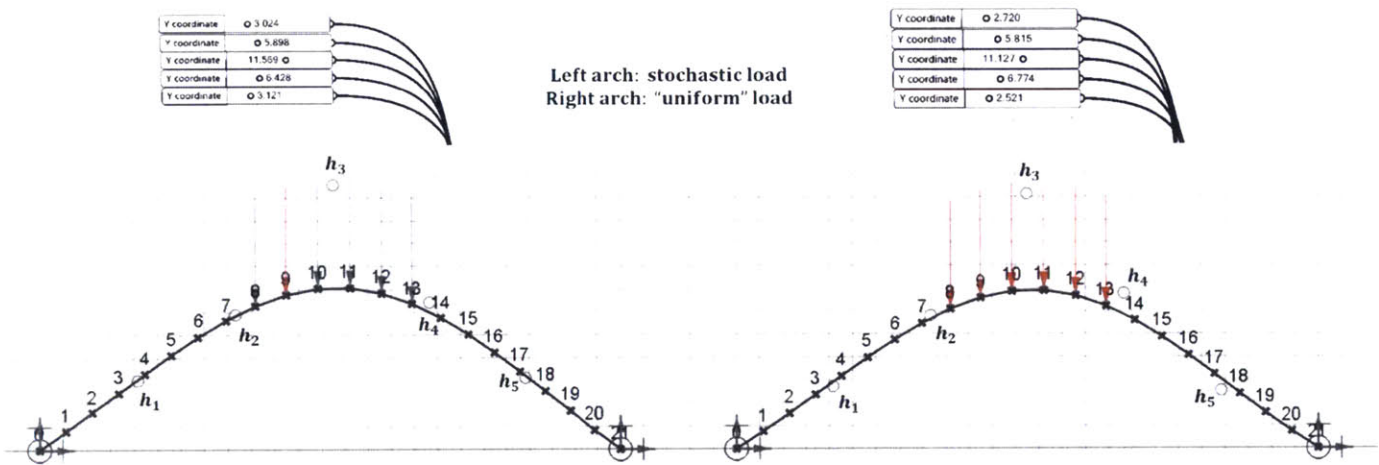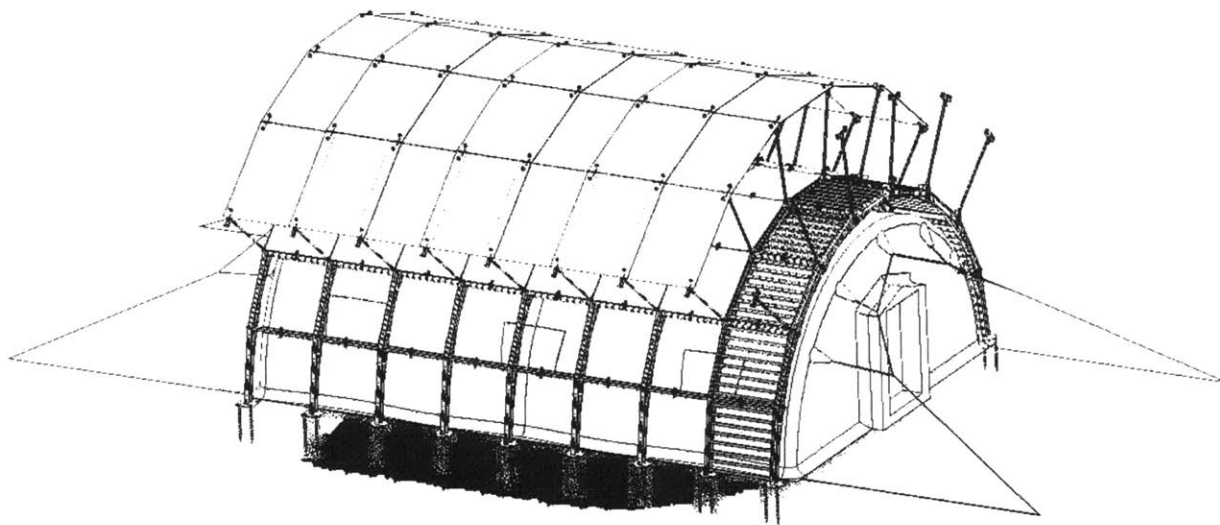

Figure 6.5

Once again, we observe the similarity between the two solutions. The arch appears relatively linear from nodes $1-7$ and $14-20$ where no loads are applied, as expected. From this observation we can reasonably assume that varying the interval over which a stochastic load can be applied will still produce an optimized shape as long as the equivalent distributed load is also applied over the same interval. We will now apply these discovered relationships to a case study where stochastic theory is relevant: the design of military defensive shelters.

41

7. Overhead Threat Protection System Case Study

The Natick Soldier Research Development and Engineering Center (NSRDEC), in collaboration with Compotech Inc. and Technical Products Inc. (TPI), is currently developing an easily deployable military shelter to defend against ballistic weaponries and other basecamp threats regularly encountered in operating zones. Termed the Overhead Threat Protection (OTP) System, the structure is an expeditionary framed system that is to be rapidly assembled by a small team of soldiers within hours of establishing an operational basecamp (OTP Fact Sheet, 2014). While several basic protective elements such as sandbags and Hesco barriers are oftentimes emplaced by early troop arrivals, these systems generally only provide protection from enemy attacks in a horizontal plane, leaving areas directly overhead unprotected. This case study briefly summarizes the current OTP System features and assess whether a modified geometry as determined through application of discussed stochastic theorem increases the performance of the system. A 3D rendering the full model erected overtop of a standard military air-beam tent is depicted below.

Figure 7.1.
(TPI Task Report, Dec. 2014)

7.1 Project Overview

The most recent OTP model features an aluminum frame adjoined to roughly resemble a semi-circle. The aluminum beams are all approximately 52" in length with a 4" deep flange-shaped cross-section and support rectangular ballistic panels, which serve as the primary defensive barrier to blasts and shrapnel. Tubular aluminum struts extend 5' outward at each connection to support the pre-detonation layer. The aluminum struts and pre-detonation layer are not included when considering the load path of the blast, as their sole purpose is to ensure the ballistic round detonates at the outer layer. A simplified cross-section of the frame design is shown below.

$W_{base} \approx 25\ ft$
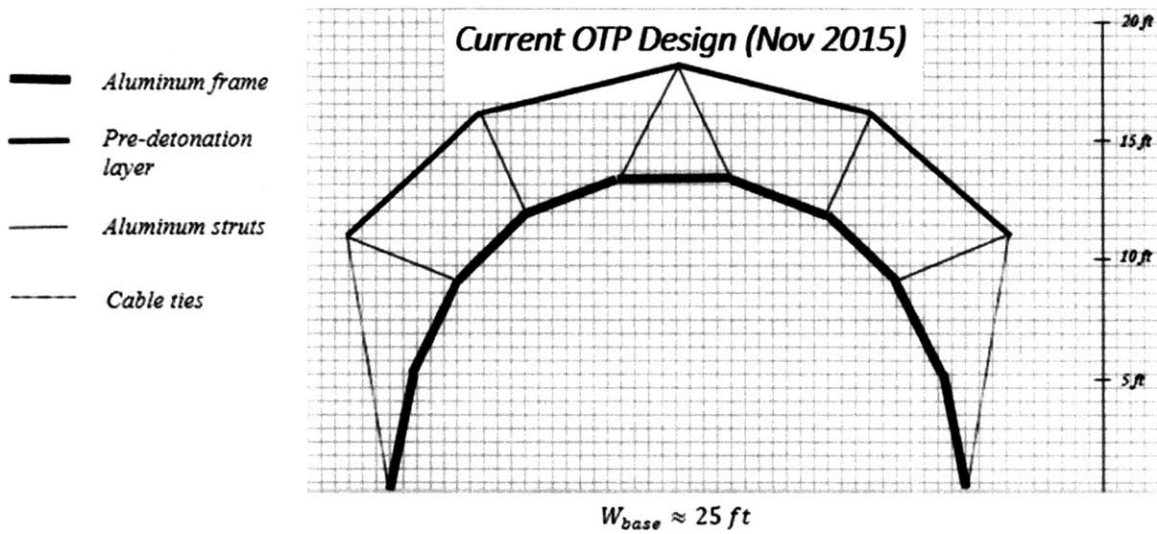
Figure 7.2.

The OTP model design allows for the frame to be erected overtop of existing, smaller military tent-like shelters. Therefore, the dimensions of these tent shelters largely drives the overall geometry of the frame. Any modifications to the geometry must respect this constraint. Additionally, the geometry of the ballistic panels is governed by the maximum weight that a person can reasonably hoist manually. Ideally, a new frame geometry would minimize changes to the ballistic panels.
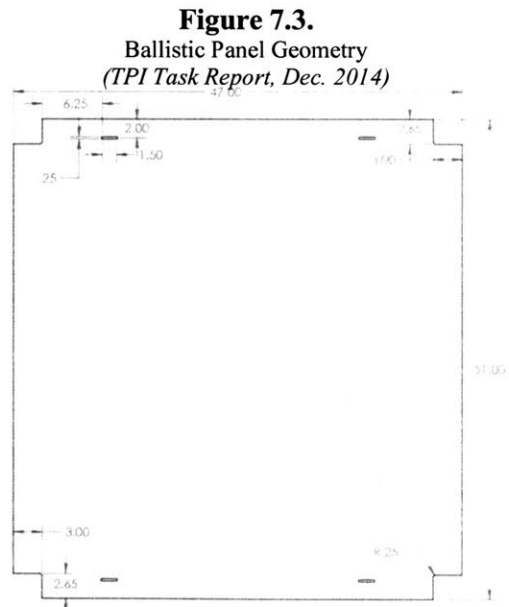
Figure 7.3.
Ballistic Panel Geometry
(TPI Task Report, Dec. 2014)

44

7.2 Defining the Geometry

We arrive at a new frame geometry by applying the theorem for stochastic loading along with the Rhino 3D models discussed in Chapter 5. We use the assumptions stated in Table 1; most importantly, that a large point load P will be randomly applied at any location on the structure. The stochastic loading theorem states that the optimal shape for this scenario is equal to that of a uniform distributed load. Segmenting the Rhino model arch into nine equal lengths of approximately the same beam length as the existing OTP model, we apply a distributed load and determine the ideal shape.
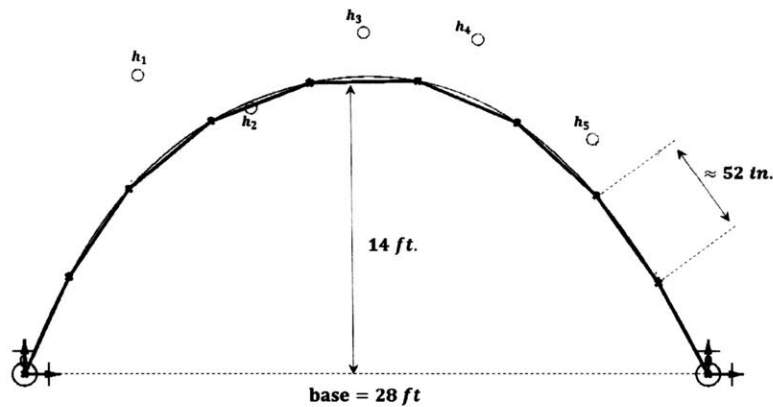
Figure 7.4. Optimum shape for segmented frame.

This optimal shape was then slightly adjusted in accordance with the project-specific restraints such as minimum ceiling height and base span. The below final frame cross-section was chosen as it minimized major changes to the individual framing elements; the beam lengths, number of beams and ballistic panels, and associated pre-detonation layer remained unchanged.
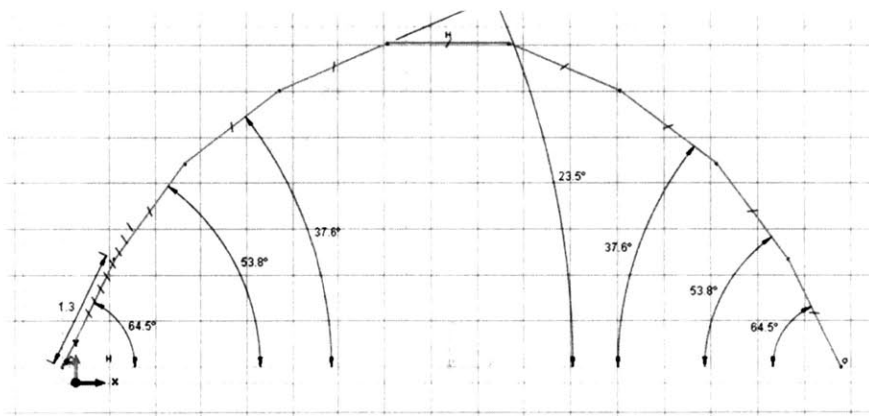

**Figure 7.5.** Geometry definition as programmed into Abaqus.

7.3 Modeling the Frame

Abaqus CAE preprocessing software was used to construct the new model and apply the design blast load. The frame members were discretized using beam elements and the ballistic panels were modeled using shell elements. These configurations were identical to previous models, with the only modification being the relative angles of each framing element. The ballistic panels attach to the frame using pinned connections at the four corners of each panel. The attachment scheme is depicted in Figure 6.6.
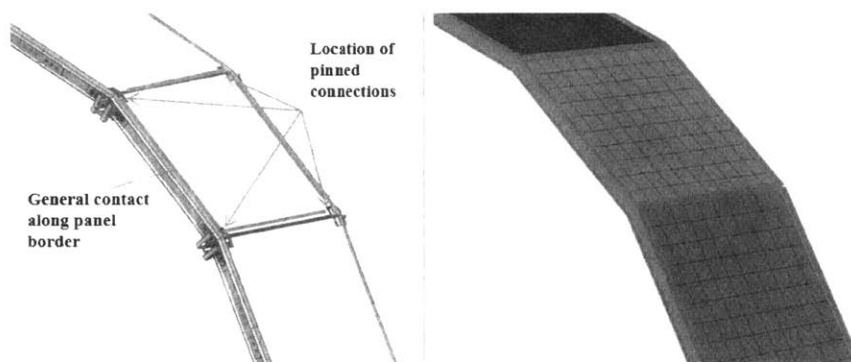

Figure 7.6. *(TPI Task Report, Dec. 2014)*

The aluminum frame was modeled using an elastic material model that includes the damage and mass damping factor. The panels were modeled using a linear stress-strain relationship that does not account for damage or plasticity, as their design assumes a stiffness large enough to transfer all applied loads to the frame. A 3D rendering of the new model in Abaqus is shown in Figure 6.7 below.
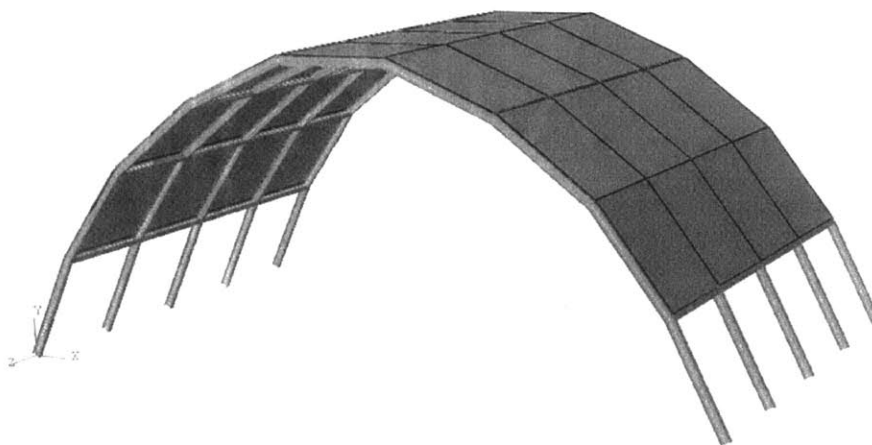

Figure 7.7. Abaqus model for redefined geometry.

46

The blast load was applied using a blast pressure function from the U.S. Army Corps of Engineers Conventional Weapons Effects Calculations (CONWEP) software synced to the Abaqus model. For a certain blast location and distance from target, the function outputs the appropriate design pressure wave (TM 5-855-1). This pressure wave was used for all previous models and therefore left unchanged when considering the new geometry. The simulated charge was located top dead center of the structure at a standoff of 5 feet as shown below.
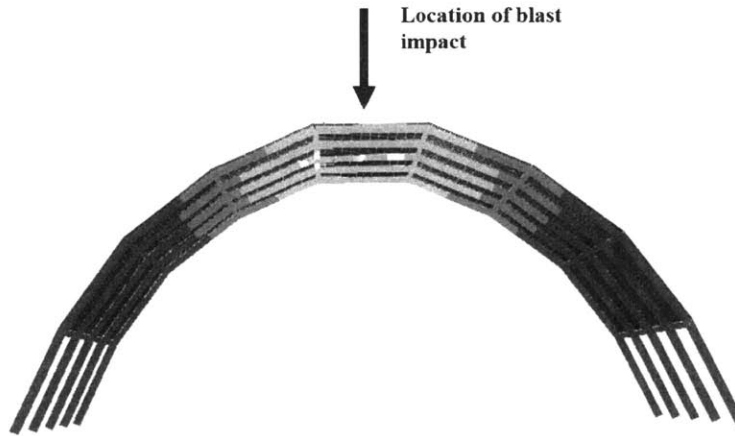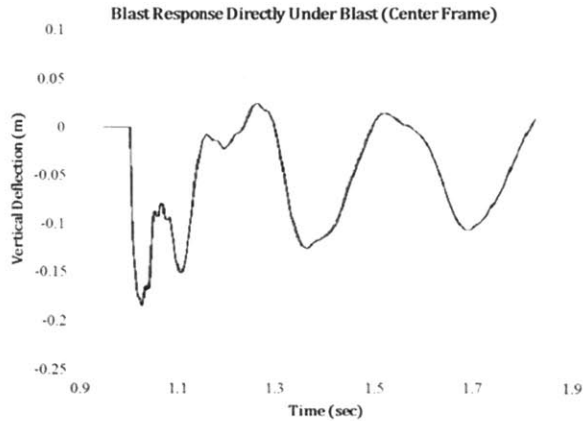

Figure 7.8.

The figure above depicts the charge location and stress distribution for a front view of the new model. The stress distribution as seen from above is illustrated below.
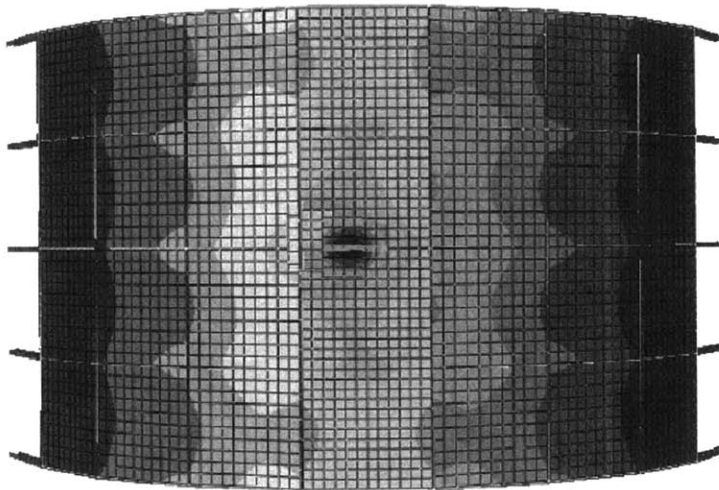
**Figure 7.9.** Stress distribution for charge location at 5' standoff.

7.4 Results

The deflection of the new model was compared to that of the original framing system. A vertical deflection over time curve is shown below that illustrates the structural response of the system to the pressure wave.

Figure 7.10. Deflection of the optimized frame.

The figure below contrasts the deflection curve with the original model, whose deflection curve is plotted in gray. The magnitude of the maximum downward deflection was approximately two-thirds of the original model deflection. Also, the period of vibration was significantly longer, which contributed to a smaller overall deflection for the new model.
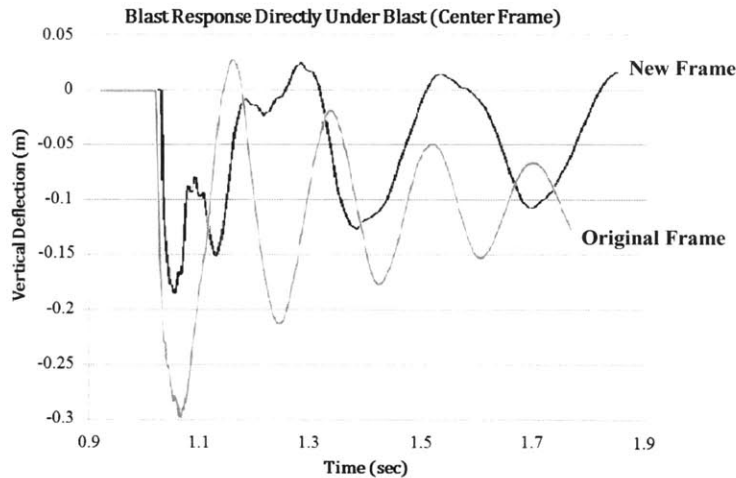
Figure 7.11. Frame performance comparison.

These results suggest that by optimizing for a stochastic load case, a higher performing geometry can be found, even when keeping the material properties and quantities constant. To continue to optimize this model, the self-weight and member dimensions should also be parametrized.

48

8. Conclusion

The contents of this thesis presented a method for determining the moment-optimized shape $y(x)$ for arched structures under unpredictable loading scenarios. The frame derivation, arch derivations, and Rhino 3D models all demonstrated the relationship between certain unpredicted loads and an equivalent guaranteed loading condition. The relationship was summarized by stating that the arch solution $y(x)$ when optimized to experience a minimum summation of the absolute value of all possible bending moment envelopes when subjected to a random point load with a likelihood of occurrence determined by a probability density function $f(x)$ is equal to the zero-moment solution for an arch subjected to a distributed load $u(x)$ when $f(x) = u(x)$.

8.1 Applicability

The application to military defensive shelters has already been discussed in the preceding chapters. However, the above-stated relationship could also prove valuable in the design of structures subjected to distributed loading conditions that are also stochastic in nature, such as wind or precipitation effects where the likelihood of required structural resistance varies throughout the structure.

8.2 Future Work

This thesis considered only the stochastic point load, and various probability density functions that could accompany the point load. However, the derivation of the funicular shape for a stochastic distributed load with a variable probability occurrence is a reasonable next step for developing the theorem further. This would increase the complexity of the derivation and possibly allow for a broader range of applicability. Also, the preceding derivations considered scenarios where the loads must occurring independently. An interesting expansion of the theorem would be to observe the changes in the optimal geometry if, for example, a point load P would occur at two randomly selected locations over the length of the arch.

Additionally, incorporating the conjecture into blast design by using a more inclusive description of a blast pressure wave instead of a point load would prove highly valuable for future research into defensive military shelters and other robust structures.

Appendix A.

Arch derivation for uniform distributed load.

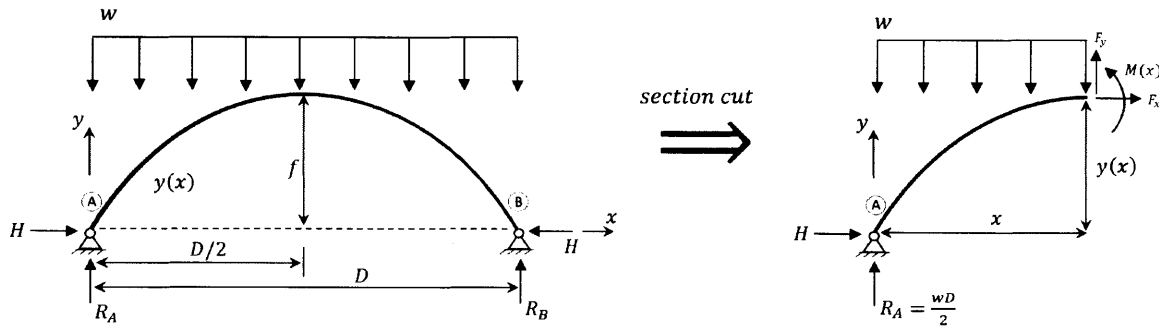Consider the symmetric two-hinged arch below subjected to the horizontally uniform distributed load w.

Figure A.1

We consider a section of length x and apply moment equilibrium at the section cut.

$$\sum M_{cut} = 0 \quad \Rightarrow \quad -M(x) + R_A * x - H * y(x) - \frac{wx^2}{2} = 0$$

Ideal arch experiences zero bending moments $\quad \Rightarrow \quad M(x) = 0$

$$-H * y(x) = \frac{wx^2}{2} - R_A * x \quad \Rightarrow \quad y(x) = \left(\frac{-xw}{2H}\right) * (x - D)$$

$$y\left(\frac{D}{2}\right) = f \quad \Rightarrow \quad \left(\frac{-\left(\frac{D}{2}\right)w}{2H}\right) * \left(\frac{-D}{2}\right) = f$$

$$f = \frac{D^2 w}{8H} \quad \Rightarrow \quad y(x) = \left(\frac{-xw}{2\left(\frac{D^2 w}{8f}\right)}\right) * (x - D)$$
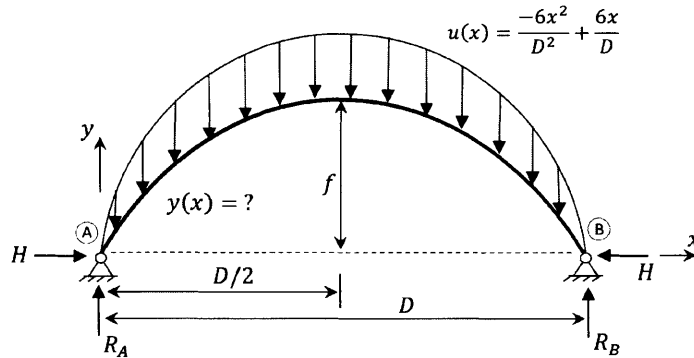
$$\Rightarrow \quad y(x) = \frac{4xf}{D^2}(D - x)$$

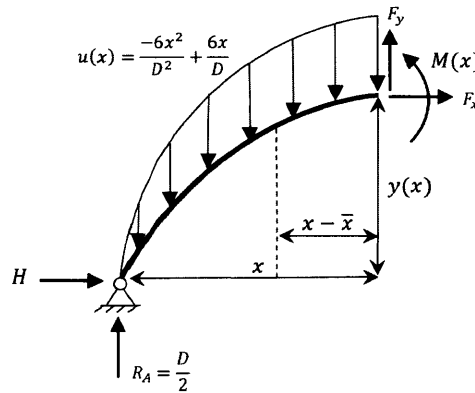$$\underline{\underline{}}$$

ANS.

50

Appendix B.

Arch derivation for non-uniform distributed load $u(x)$.

Consider the arch of unknown shape $y(x)$ subjected to the symmetric non-uniform distributed load $u(x)$ shown below.

Figure B.1

Because the area under $u(x)$ from 0 to D is equal to D, symmetry requires that $R_A = R_B = \dfrac{D}{2}$. Keeping the horizontal reaction H as a parameter, we use the method of sections.

Figure B.2

Moment equilibrium at the section cut provides the following equation,

$$-M(x) - y(x)H + \frac{Dx}{2} - (x - \bar{x})\left(\int_0^x u(x)\,dx\right) = 0$$

51

where the centroid $\bar{x}$ of the distributed load u(x) is given by:

$$\bar{x} = \frac{\int_0^x x * u(x)dx}{\int_0^x u(x)dx} = \frac{-3x^2 + 4xD}{-4x + 6D}.$$

As the ideal arch experiences no bending moment, we set $M(x) = 0$, substitute in $\bar{x}$, and solve.

$$-y(x)H + \frac{Dx}{2} - \left(x - \frac{-3x^2 + 4xD}{-4x + 6D}\right)\left(\frac{-2x^3}{D^2} + \frac{3x^2}{D}\right) = 0$$
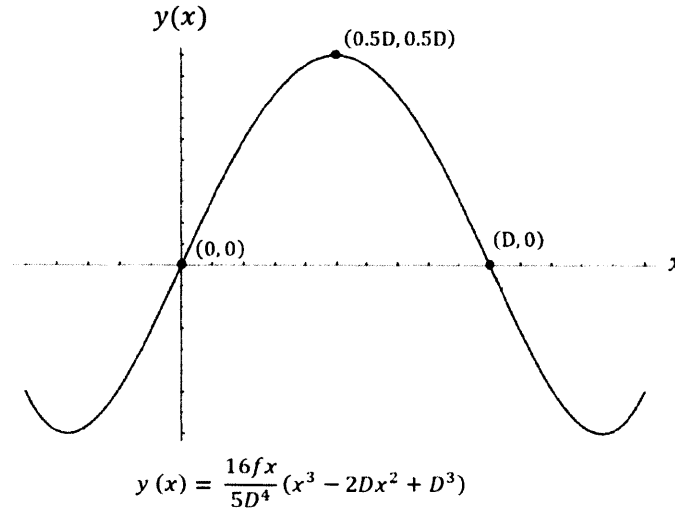
$$y(x) = \frac{1}{H}\left(\frac{Dx}{2} - \frac{x^3}{D} + \frac{x^4}{2D^2}\right)$$

$$y\left(\frac{D}{2}\right) = f \quad \Rightarrow \quad H = \frac{5D^2}{32f}$$

$$\Rightarrow \quad y(x) = \frac{16fx}{5D^4}(x^3 - 2Dx^2 + D^3)$$

<div align="right">ANS.</div>

This is the equation $y(x)$ for an ideal arch subjected to the non-uniform distributed load $u(x)$. The arch appears semi-linear close to the supports where the load concentration is low, as shown in Figure C.3.

$$y(x) = \frac{16fx}{5D^4}(x^3 - 2Dx^2 + D^3)$$

Figure B.3

Bibliography

Alves, M., and Norman Jones. *Impact Loading of Lightweight Structures.* Southampton: WIT, 2005.

Department of the Army Technical Manual TM 5-855-1, Fundamentals of Protective Design for Conventional Weapons, 3 November 1986.

Díaz, A. R., and M. P. Bendsøe. "Shape Optimization of Structures for Multiple Loading Conditions Using a Homogenization Method." *Structural Optimization 4.1* (1992): 17-22.

Horak, Karen. Overhead Protection System Fact Sheet [Unclassified. Public Affairs Office Number: 416-213]. RDECOM. October 2014.

Lockwood, E.H. "Chapter 13: The Tractrix and Catenary". *A Book of Curves.* Cambridge. 1961.

Melrose, Paul. "TPI Task Report 5, Overhead Threat Protection System Optimization." *Compotech, Inc.,* 01 December 2014.

Rozvany, G. I. N., and T. Lewiński. *Topology Optimization in Structural and Continuum Mechanics.* N.p.: n.p., n.d. Print.

"Stochastic." Merriam-Webster.com. 2011.

Timoshenko, Stephen. *Theory of Elastic Stability.* New York: McGraw-Hill, 1970.

Wolfram Research, Inc. (n.d.). WolframAlpha. http://www.wolframalpha.com.